A&A 600, A96 (2017)
DOI: 10.1051/0004-6361/201629722

Astronomy & Astrophysics

Spectral variations of the symbiotic star V407 Cygni around light maximum of the secondary Mira variable in 2012⋆

T. Iijima[1] and H. Naito[2]

[1] Astronomical Observatory of Padova, Asiago Section, Osservatorio Astrofisico, 36012 Asiago (Vi), Italy
e-mail: takashi.iijima@oapd.inaf.it
[2] Nayoro Observatory, 157-1 Nisshin, Nayoro, 096-0066 Hokkaido, Japan

Received 15 September 2016 / Accepted 7 January 2017

ABSTRACT

Context. The outburst of the symbiotic recurrent nova V407 Cyg in 2010 has been studied by numerous authors. On the other hand, its spectral variations in the quiescent stage have not been well studied yet. This paper is probably the first report for the relation between the pulsation of the secondary Mira variable and the temperature of the primary hot component for V407 Cyg.
Aims. The spectral variation in the post-outburst stage has been monitored to study the properties of this object. In the course of this work, we found some unexpected spectral variations around the light maximum of the secondary Mira variable in 2012. The relation between the mass transfer in the binary system and the pulsation of the secondary Mira variable is studied.
Methods. High- and low-resolution optical spectra obtained at the Astronomical Observatories at Asiago were used. The photometric data depend on the database of the VSNET.
Results. The secondary Mira variable reached its light maximum in 2012, when an absorption spectrum of a late-M-type giant developed and the emission line of Hδ became stronger than those of Hβ and Hγ, which are typical spectral features of Mira variables at light maxima. On the other hand, intensity ratios to Hβ of the emission lines of He I, He II, [Fe VII], etc., which obviously depended on the temperature of the hot component, rapidly varied around the light maximum. The intensity ratios started to decrease at phase about 0.9 of the periodical light variation of the Mira variable. This phenomenon suggests that the mass transfer rate, as well as the mass accretion rate onto the hot component, decreased according to the contraction of the Mira variable. However, these intensity ratios somewhat recovered just on the light maximum: phase 0.99. There might have occurred a temporal mass loss from the Mira variable at that time. The intensity ratios decreased again after the light maximum, then recovered and returned to the normal level at phase about 0.1. Since the mass transfer rate seems to have been closely related to the pulsation of the secondary component, the mass transfer in this binary system was likely due to a normal Roche-lobe overflow. If this is the case, the orbital period should be shorter than five years. Each of the Na I D1 and D2 lines had five emission and one absorption components around the light maximum. It seems that there were two pairs of mass outflows from the Mira variable with velocities of ±79 km s^{-1} and ±44 km s^{-1}. These velocities were much higher than those of mass loss from usual Mira variables.

Key words. stars: individual: V407 Cyg – novae, cataclysmic variables – binaries: symbiotic

1. Introduction

V407 Cyg was known as a symbiotic binary system consisting of a hot component and a Mira-type variable (e.g. Munari et al. 1990; Kolotilov et al. 1998). This object performed a classical-nova-like outburst in 2010 and is therefore now classified as a recurrent nova with a red giant secondary (Munari et al. 2011; Shore et al. 2011).

Detailed works have been made on the outburst in γ-ray (Abdo et al. 2010; Aliu et al. 2012), X-ray (Shore et al. 2011, 2012; Nelson et al. 2012), optical (Munari et al. 2011; Shore et al. 2011; Iijima 2015, hereafter Paper I), infrared (Munari et al. 2011), and radio wavelength regions (Peel et al. 2010; Deguchi et al. 2011; Chomiuk et al. 2012).

Meinunger (1966) found a periodical light variation with an ephemeris of

$$\mathrm{Max} = 2\,429\,710 + 745^d * E. \quad (1)$$

On the other hand, Kolotilov et al. (2003) proposed a different ephemeris based on their infrared photometry:

$$\mathrm{Max}(K) = 2\,445\,326 + 762.9^d * E. \quad (2)$$

The latter is adopted in this paper because the characteristic spectral features of Mira variables at light maxima were observed on the phase of their Max(K) in 2012. In this paper, "light maximum" means the K-band flux maximum given by this equation.

Munari et al. (1990) suggested this to have been one more periodical light variation by 43 ± 5 yr, and they hypothesized that the periodicity might have been related to the orbital motion of the binary system. Their hypothesis was rather questionable,

⋆ The reduced spectra (FITS files) are only available at the CDS via anonymous ftp to cdsarc.u-strasbg.fr (130.79.128.5) or via http://cdsarc.u-strasbg.fr/viz-bin/qcat?J/A+A/600/A96

however, because their photometric data only covered one light minimum in 1972, that is, it was not sure whether the light variation was really periodical. In addition, no spectroscopic work has confirmed the orbital motion, and recent photometric data seem to be inconsistent with their model (see Sect. 3.1).

This paper reports spectral variations of this object in the quiescent stage, in particular, those observed around the light maximum of the secondary Mira variable in 2012.

2. Observations

Low-resolution spectra, $\lambda/\Delta\lambda \cong 1000$ or 500, were obtained with a Boller & Chivens grating spectrograph mounted on the 122 cm telescope at the Asiago Astrophysical Observatory of the University of Padova. High-resolution spectra, $\lambda/\Delta\lambda \cong 15\,000$, were obtained with a Reosc Echelle spectrograph mounted on the 182 cm Copernicus telescope at the Mount Ekar station of the Astronomical Observatory of Padova. The spectra were reduced using the standard tasks of the NOAO IRAF[1] package at the Asiago Astrophysical Observatory. Spectrophotometric calibrations were made using the spectra of the standard stars HD 192281 and BD+40°4032 obtained in the same nights as the observations. A log of the observations is given in Table A.1, where UT is the universal time at start of exposure and Phase depends on the ephemeris of Kolotilov et al. (2003), Eq. (2) in the last section.

Intensities of selected emission lines relative to Hβ = 100 are given in Table A.2, where the effects of the interstellar extinction are corrected by $E(B-V) = 0.6$ (Paper I). The intensities of emission lines on a spectrum that did not cover the spectral region of Hβ are given relative to Hβ on the other spectrum obtained at the nearest time. The errors in the spectrophotometric calibrations in such a case were corrected assuming that the total fluxes in the overlapped spectral regions of the two spectra were the same. Absolute intensities of the emission line of Hβ were measured on some spectra obtained with the Boller & Chivens spectrograph in good sky condition, which are given at the bottom of Table A.2.

An absorption spectrum of a late-M-type giant developed, and most emission lines weakened around the light maximum of the Mira variable in 2012. Therefore it was difficult to measure the intensities of numerous weak emission lines because of the saw-toothed continuum. Three dots in a cell in Table A.2 means that the corresponding emission line was not detected or was not measured, while the cells in non-observed spectral regions are left blank. The observational errors in the intensities are about 10%, and the values with lower accuracy are denoted by a colon.

3. Spectral variations

3.1. Spectral features

Figure 1 shows the V and B magnitudes of V407 Cyg in 2011 and 2012. These data were uploaded in the VSNET by S. Kiyota. The expected date for the K-band flux maximum was JD 2 456 006.6: 2012 March 20, which is indicated by the vertical broken line.

The luminosities in the V and B bands rose rapidly toward the maxima then declined slowly as general light curves of Mira variables. The maxima were found around JD 2 455 960 at $V = 12.5$ mag and $B = 14.4$ mag, which was earlier than the expected date of the light maximum in the K band by phase 0.06.

[1] IRAF is distributed by NOAO for Research in Astronomy, Inc. under cooperative agreement with the National Science Foundation.

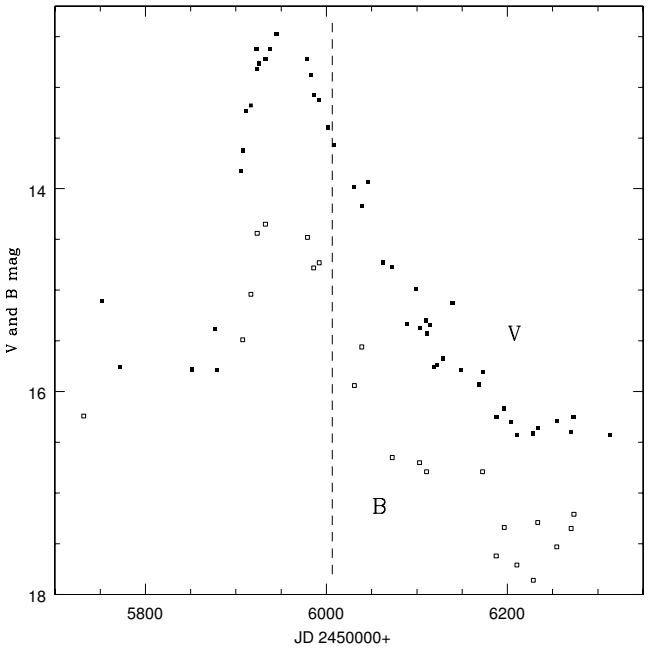

Fig. 1. V and B magnitudes of V407 Cyg in 2011 and 2012. The vertical broken line shows the expected date for the K-band flux maximum.

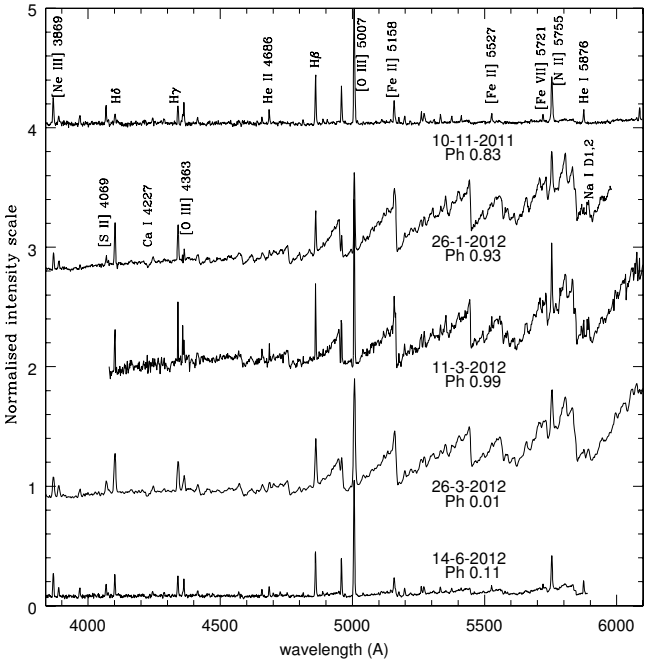

Fig. 2. Tracings of selected spectra of V407 Cyg obtained in 2011 and 2012.

If the long-term light variation proposed by Munari et al. (1990) were really periodical, the expected peak luminosity on the light maximum in 2012 should be $B = 15.4$ mag (Fig. 1 in their work), that is, our result disagrees by 1 mag.

Figure 2 shows tracings of selected spectra obtained in 2011 and 2012. The top spectrum was obtained on 2011 November 10: JD 2 455 876.4 when the Mira variable was still faint (Fig. 1). The spectral features were similar to those in the nebular stage of the outburst in 2010 (Paper I). The prominent emission lines were due to H I, He I, He II, [O III], [N II], [Ne III], [Fe II], [S II],

[Fe VII], etc. The absorption bands of TiO molecules were weak and the emission line of Hδ was weaker than those of Hγ and Hβ.

The second spectrum was obtained on 2012 Jan. 26: JD2 455 953.3, that is, nearly at the peak of V mag. The spectral features of a late-M-type giant developed with deep absorption bands of TiO molecules and the broad absorption line of Ca I 4227. The emission line of Hδ became stronger than those of Hγ and Hβ, and the emission lines of Na I D1 and D2 were detected. The unusual high intensity of the emission line of Hδ is a typical spectral feature of Mira variables at light maxima. The emission line of Hβ weakened but did not disappear, which means that the emission from the nebulosity ejected during the outburst in 2010 was still prominent. When Herbig (1960) observed this object, only Hδ was seen in emission. His observation was probably made on a light maximum of the Mira variable, and moreover, there was no circumstellar nebulosity at that time. The emission lines of He I, He II, [O III], [N II], [Ne III], etc. weakened.

The third spectrum was obtained on 2012 March 11: JD 2 455 997.5, that is, nearly on the date of light maximum. The spectral features of the late-M-type giant were clearly visible. The emission lines of H I, He I, He II, [O III], [N II], etc. somewhat strengthened, however. This phenomenon is discussed in the next subsection.

The fourth spectrum was obtained on 2012 March 26: JD 2 456 012.7, when the V mag was 1.2 mag below maximum (Fig. 1), while the K-band flux was possibly still nearly at maximum. The spectral features of the late-M-type giant were clearly visible and the emission lines weakened again.

The bottom spectrum was obtained on 2012 June 14: JD 2 456 092.6, when the V mag was 2.7 mag below maximum (Fig. 1). The spectral features of the late-M-type giant weakened and the emission lines strengthened. The emission line of Hδ was still stronger than that of Hγ.

3.2. Intensity variations of the emission lines

The intensities of selected emission lines relative to Hβ = 100 are given in Table A.2. The upper panel of Fig. 3 shows the intensities of prominent emission lines relative to Hβ in logarithmic scale, and the lower panel shows the intensity ratio of I(Hδ)/(Hβ) in linear scale.

The intensity ratios to Hβ of the emission lines of He I, He II, and [Fe VII] decreased on JD 2 455 953, phase 0.93, and recovered on JD 2 455 998, phase 0.99, then decreased again on JD 2 456 013, phase 0.01. The emission lines of [Ca V] and [Fe VI] showed similar variations (Table A.2). When we compare the heights of the emission lines of [O III] 5007, 4959 and [N II] 5755 with the depths of the nearby TiO absorption bands on the tracings in Fig. 2, it is easy to note their variations in intensity. Their variations, however, were nearly compensated by that of Hβ, and no significant variation was seen in the intensity ratios to Hβ (Fig. 3).

The intensity ratios to Hβ of emission lines such as He I, He II, [Fe VII], and [Ca V] depend on the UV radiation from the hot component in the binary system. Their fading suggests that the temperature of the hot component decreased in the phases around the light maximum of the Mira variable. The mass accretion rate onto the hot component probably decreased as a result of the decreasing mass transfer rate in the binary system. If the secondary Mira variable filled or overflowed its Roche lobe when expanded, but was well detached from the Roche lobe when contracted around light maxima, such a phenomenon may have been possible to occur.

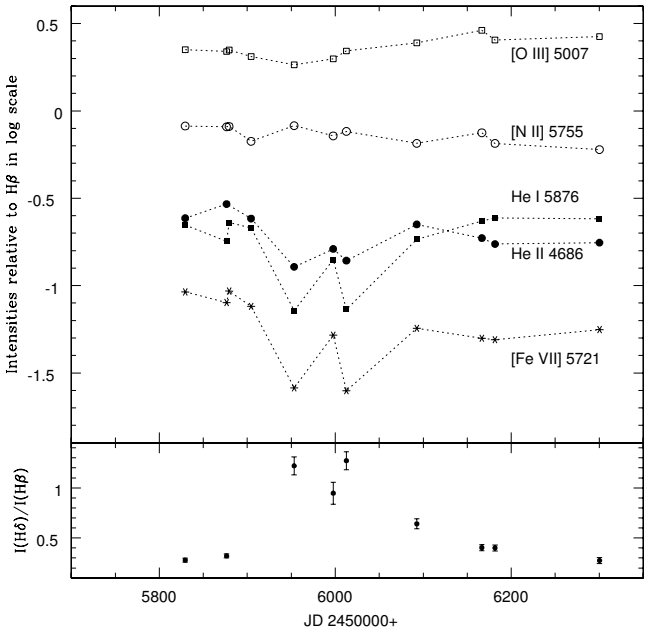

Fig. 3. Intensities of selected emission lines relative to Hβ and intensity ratio of I(Hδ)/(Hβ).

The temporal recovering of the intensity ratios of the emission lines just on the light maximum JD 2 455 998 (Fig. 3) is rather uncertain, because we have only one observation. Model calculations for mass loss from Mira variables made by Wood (1979) showed that a shock wave propagated once per period and occasional ejections of shell occurred in the isothermal condition as a result of coalescing of the shocks. There might have occurred such a sudden mass loss from the secondary Mira variable at that time if the recovering was real. Further works are needed to examine this phenomenon.

The emission line of Hδ became stronger than those of Hβ and Hγ (Fig. 3), which is a well-known spectral feature of Mira variables at light maxima. The intensity ratio I(Hδ)/(Hβ) did not become so high, however because the emission line of Hβ from the circumstellar nebulosity was still prominent. The decreasing of the intensity ratio I(Hδ)/(Hβ) just on the light maximum, JD 2 455 998, suggests that the H I emissions from the circumstellar nebulosity strengthened.

3.3. Emission lines of Na I D1 and D2

When the spectrum of the late-M-type giant developed, the emission lines of Na I D1 and D2 became prominent (Fig. 2, Table A.2). These lines were most likely related to the Mira variable because they were very weak when the nebular emission lines were dominant, as seen in the top spectrum in Fig. 2.

The emission lines of Na I D1 and D2 were observed on some Mira variables, for instance, χ Cyg (Sanner 1977). Sanner (1977) found simple P Cygni-type profiles of these lines, while those of V407 Cyg were more complex. Figure 4 shows the profiles of Na I D1 and D2 on 2012 March 11, that is, a part of the third spectrum in Fig. 2. As seen in the figure, each of Na I D1 and D2 had five emission and one absorption components. The emission components are indicated by the letters a–e with suffix 1 or 2. The same letters are given to the counterparts having close radial velocities, and the suffix shows whether the component depends on Na I D1 or D2. The absorption components of Na I D1 and D2 are indicated by ab1 and ab2. The heliocentric

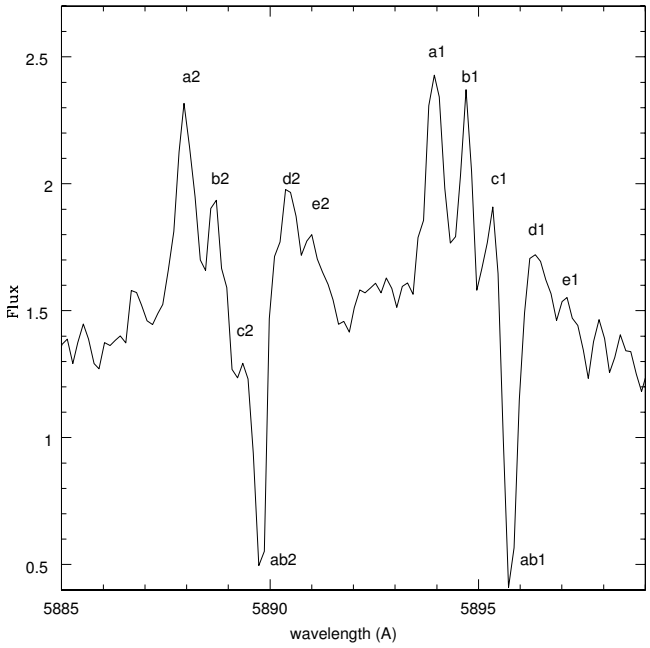

Fig. 4. Detailed profiles of Na I D1 and D2 on 2012 March 11.

Table 1. Radial velocities in km s^{-1} of emission and absorption components of Na I D1 and D2, and those of He I 5876 and [N II] 5755.

ID	D1	D2
a	–100.4	–101.8
b	–61.7	–65.2
c	–30.2	–27.0
d	+22.7	+25.5
e	+59.5	+53.2
ab	–8.1	–9.2
He I 5876	–22.5	
[N II] 5755	–25.0	

radial velocities of the emission and absorption components are given in Table 1, where the radial velocities of the emission lines of He I 5876 and [N II] 5755 are also given. The observational errors are about ±1 km s^{-1}.

The absorption components were probably due to the interstellar matter because no absorption or emission components in the spectrum of this object had similar radial velocity (Paper I). It seems that there were two pairs of the emission components, respectively, one of those was a1,2 and e1,2 and the other was b1,2 and d1,2, because those were in symmetry with respect to the same central velocity. The mean radial velocity of the centre of symmetry of these pairs was -21 ± 2 km s^{-1}, which may have reflected the radial velocity of the Mira variable. Unfortunately, we are unable to determine at the present time whether this velocity is slightly different from the mean radial velocity of the emission lines He I 5876 and [N II] 5755: -24 ± 2 km s^{-1}, or if these two velocities agree with each other in the range of the observational errors.

The multiple emission components of Na I D1 and D2 lines suggest that there were two symmetric gas outflows with velocities of $\pm 79 \pm 2$ km s^{-1} and $\pm 44 \pm 2$ km s^{-1}. These velocities are much higher than those of gas outflows observed in usual Mira variables. For example, the survey of the outflow velocities from nearby Mira variables (Young 1995) showed that most of them were lower than 10 km s^{-1}. Dickinson et al. (1975) studied the double-peaked profiles of OH maser emissions of long-period variables. The relation between the period and the separation of the peaks, Fig. 1 in their work, gives a separation of peaks of about 40 km s^{-1} for the period 762.9 day, that is, the outflow velocity is 20 km s^{-1}. This velocity is still much lower than those observed in V407 Cyg. The companions of the emission components c1 and c2 were possibly merged in the absorption components. If this was the case, there might have been one more weak pair of outflow with velocities of about ±8 km s^{-1}, which is consistent with the outflow velocities of usual Mira variables.

The high velocity outflows of V407 Cyg were probably accelerated by the radiation of the hot component. However, a detailed work for the geometry of the outflows is beyond the scope of this paper.

4. Discussion

Some notable variations were observed in the spectrum of V407 Cyg around the light maximum of the secondary Mira variable in 2012. The spectrum of a late-M-type giant developed and the emission line of Hδ became stronger than those of Hβ and Hγ, which have been observed at light maxima of usual Mira variables. On the other hand, the intensity ratios to Hβ of the emission lines of He I, He II, [Fe VII], etc., which were related to the temperature of the hot component, also varied around the light maximum. The mass transfer rate in the binary system, as well as the mass accretion rate onto the hot component, may have decreased according to the contraction of the Mira variable in the phases around the light maximum. The intensity ratios, however, seem to have somewhat recovered just on the light maximum (Fig. 3). An occasional mass loss from the Mira variable, which was expected in the model calculations of Wood (1979), might have occurred at that time.

The spectral variations observed in this work suggest that the mass transfer rate in the binary system varied according to the pulsation of the Mira variable. Munari et al. (1990) proposed an orbital period of 43 ± 5 yr for the binary system of V407 Cyg. The mass transfer in such a long-period binary system should be due to a capture of the stellar wind or a mechanism called "wind Roche-lobe overflow" (Mohamed & Podsiadlowski 2012). It seems to be unlikely, however, that the mass transfer rates by such mechanisms were closely related to the pulsation of the Mira variable. Since our results suggest a connection between the mass transfer and the pulsation of the Mira variable, the mass transfer in the binary system of V407 Cyg may be more probably due to a normal Roche-lobe overflow. If the Mira variable overflows its Roche lobe when it expands, the orbital period is likely shorter than five years with reasonable masses of the primary and secondary components. As seen in Fig. 3, the temperature of the hot component seems to have varied according to the pulsation of the Mira variable without a great time lag. This phenomenon suggests that the binary system is probably still more compact. Further works to search the periodicity in the photometric and spectroscopic phenomena are necessary.

The multiple emission components of Na I D1 and D2 lines suggest that there were high velocity outflows in this binary system. The outflows were probably located around the Mira variable, but they were very likely accelerated with the radiation of the hot component. The detailed properties of the high-velocity outflows, however, are not known yet.

Acknowledgements. I am grateful to M. Kato and I. Hachisu for the useful discussions and suggestions. Thanks are also due to S. Kiyota for the photometric data of V407 Cyg.

References

Abdo, A. A., Ackermann, M., Ajello, M., et al. 2010, Science, 329, 817
Aliu, E., Archambault, S., Arlen, T., et al. 2012, ApJ, 754, 77
Chomiuk, L., Krauss, M. I., Rupen, M. P., et al. 2012, ApJ, 761, 173
Deguchi, S., Koike, K., Kuno, N., et al. 2011, PASJ, 63, 309
Dickinson, D. F., Kollberg, E., & Yngvesson, S. 1975, ApJ, 199, 131
Herbig, G. H. 1960, ApJ, 131, 632
Iijima, T. 2015, AJ, 150, 20 (Paper I)
Kolotilov, E. A., Munari, U., Popova, A. A., et al. 1998, Astron. Lett., 24, 526
Kolotilov, E. A., Shenavrin, V. I., Shugarov, S. Yu., & Yudin, B. F. 2003, Astron. Rep., 47, 777
Meinunger, L. 1966, Mitteilunger über Veränderliche Sterne, Band 3, Heft 4
Mohamed, S., & Podsiadlowski, Ph. 2012, Baltic Astron. 21, 88
Munari, U., Margoni, R., & Stagni, R. 1990, MNRAS, 242, 653
Munari, U., Joshi, V. H., Ashok, N. M., et al. 2011, MNRAS, 410, L52
Nelson, T., Donato, D., Mukai, K., Sokoloski, J., & Chomiuk, L. 2012, ApJ, 748, 43
Peel, M. W., Gawronski, M. P., Browne, I. W. A., et al. 2010, ATel, 2905, 1
Sanner, F. 1977, ApJ, 211, L35
Shore, S. N., Wahlgren, G. M., Augusteijin, T., et al. 2011, A&A, 527, A98
Shore, S. N., Wahlgren, G. M., Augusteijin, T., et al. 2012, A&A, 540, A55
Wood, P. R. 1979, ApJ, 227, 220
Young, K. 1995, ApJ, 445, 872

Appendix A: Addditional tables

Table A.1. Log of spectroscopic observations of V407 Cyg.

Date		UT	JD	Phase	exp. s	Inst.	Range nm	ID No.
2011								
Sept.	24	23:22	5829.5	0.77	300	B&C	360–590	12665
Sept.	24	23:29	″	″	2400	″	″	12666
Sept.	25	01:06	5829.6	″	300	″	510–740	12675
Sept.	25	01:13	″	″	1800	″	″	12676
Nov.	10	22:11	5876.4	0.83	1800	″	375–609	13385
Nov.	13	21:34	5879.4	0.83	2400	Ech	428–780	52703
Dec.	8	20:30	5904.4	0.87	1200	″	″	52925
2012								
Jan.	26	17:54	5953.3	0.93	1200	B&C	360–590	15970
March	11	4:15	5997.7	0.99	1800	Ech	428–780	53518
March	26	3:40	6012.7	0.01	60	B&C	370–780	19414
March	26	3:43	″	″	600	″	″	19415
June	14	1:46	6092.6	0.11	300	″	360–590	21563
June	14	1:53	″	″	1200	″	″	21564
June	15	1:42	6093.6	0.11	1200	″	565–800	21599
Aug.	27	2:01	6166.6	0.21	2400	″	360–590	24211
Aug.	28	1:26	6167.6	0.21	1800	″	560–795	24260
Sept.	11	1:41	6181.6	0.23	1800	″	370–605	24564
2013								
Jan.	7	18:28	6300.3	0.38	2400	″	″	27551

Notes. UT: universal time at start of exposure. JD: Julian date – 2 450 000. Phase: $2\,445\,326 + 762.9 * E$ (Kolotilov et al. 2003). The spectral resolution for 19414 and 19415 is 500 and that for the other spectra of B&C is 1000.

Table A.2. Intensities of selected emission lines relative to Hβ = 100 corrected by $E(B-V) = 0.6$.

Date 2011/2012	Sep. 24	Sep. 25	Nov. 10	Nov. 13	Dec. 08	Jan. 26	Mar. 11
JD 2 450 000+	5829.5	5829.6	5876.4	5879.4	5904.4	5953.3	5997.7
Phase	0.77	0.77	0.83	0.83	0.87	0.93	0.99
[O II] 3726	38.0					29.2	
[Ne III] 3868	81.6		86.7			58.8	
H I 3889	28.8		31.9			36.1	
Hϵ [Ne III] 3968	30.6		33.5			15.1	
[S II] 4069	53.7		51.9			34.7	
[S II] 4076	12.0:		14.0:			12.2	
Hδ	27.9		32.1			122.0	94.7:
[Fe II] 4244, 4245	19.3		16.0			23.9	...
[Fe II] 4287	15.5		12.9			10.1	...
Hγ	47.1		46.9	...	45.3	101.8	69.6
[O III] 4363	47.2		50.5	...	46.7	25.9	30.0
[Fe II] 4415	22.4		17.0	...		27.5	6.1:
[Fe II] 4452	6.4		3.4:	...		22.5:	...
[Fe II] 4458	9.5		7.8:	...		15.7:	...
HeI 4471, [Fe II]4470	9.8		5.0:	...	4.6		...
[Fe III]4574, MgI4571	9.2		7.3:	...		...	...
[Fe III] 4658	15.4		13.4	...	15.0	15.9	13.4
He II 4686	24.3		29.3	...	24.2	12.8	16.2
[Fe III] 4701	7.5		...	...	8.0	13.2:	6.8
[Fe II] 4814	10.6		9.2	10.2	7.9	4.6	5.0:
Hβ	100		100	100	100	100	100
[Fe II] 4890	9.8		9.4	7.9	6.9	9.2	4.8:
[O III] 4959	64.5		64.8	71.1	72.2	38.6	57.2
[O III] 5007	224		219	223	205	184	198
[Fe II] 5043	5.4		4.1:	6.1:	11.8:	13.8	3.8:
[Fe VI] 5147	5.8		7.1	7.0	7.5	...	...
[Fe II] 5159	46.5		40.7	41.8	36.1	43.2:	21.3
[Fe VI] 5177	8.9		7.4	10.2	9.7	2.6:	5.8
[N I]5198, [Fe II]5199	14.9		15.7	13.8	18.8	12.7	15.8:
[Fe II] 5262	21.8		18.5	18.5	17.1	19.6:	8.8
[Fe III] 5270	25.1		25.1	25.8	26.2	20.0	14.7:
[Ca V] 5309	5.2		7.3	4.6	8.6	0.4	3.6
[Fe II] 5334	16.4		14.4	13.2	13.9	11.6	8.8
[Fe II] 5376	12.9		10.1	8.0	8.4	9.7	...
He II, [Fe II] 5412	9.1		8.7	8.4	6.7	1.0:	1.8:
[Fe II] 5527	15.3	15.0	15.2	12.5	13.0	6.2:	8.4
[Fe VII] 5721	9.2	8.0	8.0	9.3	7.6	2.6	5.2
[N II] 5755	81.9	86.2	81.1	81.4	67.0	82.3	72.0
He I 5876	22.2	20.9	17.9	23.0	21.4	7.2	14.1
Na I 5890	...	...	0.9:	...	2.4	16.9	6.1
Na I 5896	...	...	0.2:	...	2.3	17.4	6.8
[Fe VII], [Ca V] 6086		14.4	13.9	13.2	10.1		6.7
[O I] 6300		113.4		136.1	128.6		94.7
[S III] 6310		11.5		16.2	23.2		7.9
[O I] 6364		38.2		47.6	53.6		31.9
[N II] 6548		162		197	156		153
Hα		444		518	620		632
[N II] 6584		494		598	417		471
[Ni II] 6668		10.9		7.2:			...
He I 6678		9.1		7.7:			...
[S II] 6717		11.0:		14.9	15.3		13.3
[S II] 6731		22.8		33.6	44.7		29.7
He I 7065		10.4		10.2:			13.9:
[Ar III] 7135		12.7		18.4:			12.9:
[Fe II] 7155		57.4		...			57.6:
Hβ: 10^{-12} erg cm^{-2} s^{-1}	0.82		0.74				

Table A.2. continued.

Date 2012/2013	Mar. 26	Jun. 14	Jun. 15	Aug. 27	Aug. 28	Sep. 11	Jan. 07
JD 2 450 000+	6012.7	6092.6	6093.6	6166.6	6167.6	6181.6	6300.3
Phase	0.01	0.11	0.11	0.21	0.21	0.23	0.38
[O II] 3726	23.2			68.6		61.3	39.5
[Ne III] 3868	75.6	85.7		101.6		58.9	82.9
H I 3889	45.9	34.0		32.8		21.5:	25.8
Hϵ [Ne III] 3968	27.1	36.6		35.3		25.1:	27.5
[S II] 4069	43.9	45.7		58.9		52.1	37.0
[S II] 4076	...	13.3		16.9:		14.5:	17.2:
Hδ	127.2	64.1		40.4		40.1	27.5
[Fe II] 4244, 4245	18.0	13.6		16.5		12.5	9.3
[Fe II] 4287	...	12.7		13.7		13.2	8.2
Hγ	91.5	54.9		51.9		49.4	43.3
[O III] 4363	29.7:	44.2		63.8		59.2	30.2:
[Fe II] 4415	20.9	14.6		17.5		13.2	13.7
[Fe II] 4452	6.7:	4.2:		4.9:		7.5:	6.7
[Fe II] 4458	10.4:	7.4		3.9:		...	...
HeI 4471, [Fe II]4470	2.2:	6.2		6.3		5.9	6.7:
[Fe III]4574, MgI 4571	10.8:	10.1		7.7:		6.5	10.9
[Fe III] 4658	16.1:	13.4		15.6		18.7	17.4
He II 4686	13.9	22.4		18.7		17.3	17.6
[Fe III] 4701	5.7	8.0		7.1		4.5	7.5
[Fe II] 4814	2.7:	8.0		8.5		6.8	9.7
Hβ	100	100	100	100	100	100	100
[Fe II] 4890	...	6.5:		8.6		7.1:	4.5:
[O III] 4959	40.8:	75.4		95.9		77.3	76.5
[O III] 5007	220	245		290		255	266
[Fe II] 5043	6.5	4.3		4.3		6.6	2.2:
[Fe VI] 5147	...	6.0		5.7		5.6	...
[Fe II] 5159	27.3:	28.1		35.1		34.1	28.9
[Fe VI] 5177	3.3:	8.5		7.1		6.8	8.4
[N I]5198, [Fe II]5199	12.5	18.5		19.9		18.6	25.2
[Fe II] 5262	22.9	15.0		14.8		14.5	13.3
[Fe III] 5270	15.9	18.8		19.5		18.9	16.7
[Ca V] 5309	2.0	3.5		3.3		4.0	2.9
[Fe II] 5334	6.0	9.2		10.0		9.4	6.4
[Fe II] 5376	5.1:	7.3		8.8		8.2	6.6
He II, [Fe II] 5412	...	3.4		4.9		6.9	6.4
[Fe II] 5527	7.0:	9.4		9.8		11.3	6.9
[Fe VII] 5721	2.5	5.7	5.5	5.0	5.6	4.9	5.6
[N II] 5755	76.3	65.2	69.5	75.0	76.8	65.1	60.1
He I 5876	7.3	18.4	18.7	23.4	23.6	24.4	24.1
Na I 5890	10.9:		2.3	0.8	1.5	0.6:	...
Na I 5896	8.0:		1.7	0.6	1.3	0.4:	...
[Fe VII], [Ca V] 6086	3.7		10.1		9.9		
[O I] 6300	92.1		96.0		101.0		
[S III] 6310	...		11.7		11.0		
[O I] 6364	18.7:		30.7		34.6		
[N II] 6548	147		169		164		
Hα	513		467		438		
[N II] 6584	467		505		511		
[Ni II] 6668	...		3.7:		10.0		
He I 6678	...		5.0:		10.7		
[S II] 6717	...		6.4:		10.6		
[S II] 6731	22.1		30.0		31.2		
He I 7065	26.9:		11.3		9.4		
[Ar III] 7135	4.5:		12.4		12.2		
[Fe II] 7155	51.4		53.8		50.8		
Hβ: 10^{-12} erg cm^{-2} s^{-1}	0.64:	0.68		0.57		0.64:	